Mirage: Exploring Interaction Modalities Using Off-Body Static Electric Field Sensing

Adiyan Mujibiya
The University of Tokyo
7-3-1 Hongo, Bunkyo-ku, Tokyo 113-0033, Japan
adiyan@acm.org

Jun Rekimoto
The University of Tokyo
Sony Computer Science Laboratories, Inc.
rekimoto@acm.org

ABSTRACT
Mirage proposes an effective non body contact technique to infer the amount and type of body motion, gesture, and activity. This approach involves passive measurement of static electric field of the environment flowing through sense electrode. This sensing method leverages electric field distortion by the presence of an intruder (e.g. human body). *Mirage* sensor has simple analog circuitry and supports ultra-low power operation. It requires no instrumentation to the user, and can be configured as environmental, mobile, and peripheral-attached sensor. We report on a series of experiments with 10 participants showing robust activity and gesture recognition, as well as promising results for robust location classification and multiple user differentiation. To further illustrate the utility of our approach, we demonstrate real-time interactive applications including activity monitoring, and two games which allow the users to interact with a computer using body motion and gestures.

Author Keywords
Electric Field sensing; Off-body sensing; Motion detection; Activity recognition; Gesture recognition;

ACM Classification Keywords
H.5.2 [User Interfaces]: Input devices and strategies;

INTRODUCTION
Electronic devices with significant computational resources can now be carried mobile and becoming more ubiquitous. Such advancements lead to a growing research interest in new human-computer interfaces that go beyond the traditional paradigm of keyboard, mouse, and touch screen, including explorations on leveraging human body motion, gesture, and activity to support always-available computing, either with devices that people carry on their bodies, or using devices embedded in the environment.

UIST'13, October 8–11, 2013, St. Andrews, United Kingdom.

http://dx.doi.org/10.1145/2501988.2502031

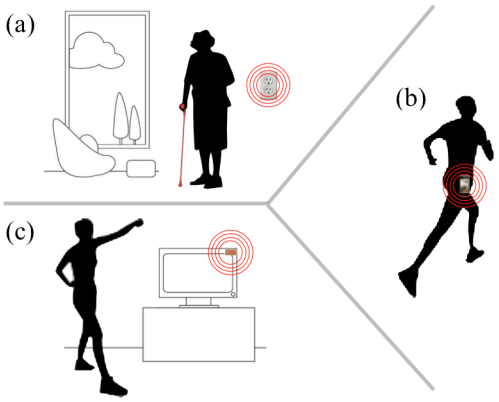

Figure 1. *Mirage* infers the type and amount of body motion, gesture, and activity by passively measuring ambient (off-body) static electric fields. Here we show three configurations representing supported application domains: (a) environmental sensor, (b) mobile sensor, and (c) peripheral-attached sensor.

Electric Field (EF) sensing offers strategic solution for these challenges, and recently has gain significant attention due to the availability of inexpensive electronic components to measure the relatively small signals. However, it is difficult to acquire stable and easily interpretable signal which is important to aggregate meaningful contextual information in a *passive* (for low-power and simple hardware implementation) and *non body contact* configuration (for broader support in interaction modalities). Our research addresses these issues to make EF sensing more accessible to interface designers.

We present *Mirage*, a novel sensing approach to infer the amount and type of body motion, gesture, and activity using non body contact technique leveraging human-generated body charge. *Mirage* utilizes passive (i.e., no additional signal transmission) static EF measurement through an electrode placed at a distance from the subject. Human body will induce EF distortions when performing motions. We leverage this phenomenon and show that human body motion and gesture produce significant signals at useful ranges. *Mirage* sensing principles robustly extract these signals by leveraging the design of sample-and-hold circuit in the Successive Approximation Register (SAR) Analog to Digital Converter (ADC), which is widely used in microcontrollers boards such as Arduino [4].

Mirage software system incorporates signal processing and analysis approaches to provide contextual information such as: 1) presence detection, 2) amount and type of body motion, whole-body gesture, and activity, 3) location classification, and 4) multiple user differentiation.

Mirage sensing approach requires no instrumentation to the user or electrical infrastructure. It can be configured as an environmental, mobile, or peripheral-attached sensor (Figure 1). Each setup represents different application domains with broad interaction modalities. The sensing hardware consumes as low as 1.8 μW, and only requires a single analog input of an off-the-shelf microcontroller. Moreover, the sensing unit met safety requirements, and inexpensive in both hardware and software.

The sensing technology proposed is *scalable,* e.g., motion and activity sensing is equally effective across user (no requirement for user dependent training) and across environment (across buildings and outdoor). The gesture recognition and location classification system requires minimal user dependent training and incorporates real-time segmentation and machine learning-based classification.

The specific contributions of this paper are:

1) Proposal and development of a novel non body contact passive static electric field sensing. This technique leverages the design of ADC in an off-the-shelf microcontrollers such as Arduino.
2) Description of the theory of operation and detailed implementation of the sensing system, including signal acquisition, signal processing, event detection, segmentation, feature extraction, and classification.
3) Presentation of results from a series of controlled experiments to demonstrate the usability of our technology including: a) activity recognition, b) whole-body gesture recognition, c) location classification, and d) multiple user differentiation. We also demonstrate *Mirage*'s usage in real-time interactive applications.

RELATED WORK

Motion sensing systems have been used in applications such as activity and gesture recognition, health and wellness monitoring, security and surveillance systems, and also elder care. Conventional methods have largely used infrared systems, computer vision techniques, or inertial sensors.

Infrared systems have been widely used for human motion sensing. However, these systems have limitations in high-rate of false detections and artifacts caused by the presence of illumination sources inside the surveillance area. Such systems often only detect the presence of a subject, and relatively difficult to infer activity or gesture. Also, these systems are impractical for deployment in large areas because they typically require significant power.

Alternatively, computer vision and depth sensing systems (e.g. Kinect [29] and Motion Capture system [26]) have been used for detecting body motion and gesture, mainly because they are gradually becoming inexpensive, and at the same time provide accurate measurement of three-dimensional sensing of body segments. The commercial success of these devices and the advancements of computer vision in general have stimulated the ideas of consumers and researchers alike, and have led to rapid growth in explorations (e.g. see [28]). Computer vision based approaches also provide measurement methods that do not require the user to wear any additional device, such as [16]. However, these approaches are limited in the potential scale of deployment due to their associated installation burden and cost. Also, these systems typically suffer from occlusion and require line-of-sight.

Body-mounted inertial sensors have been used extensively for the detection of human body motion and activity recognition [2,9,12,17,20]. These techniques often require users to place the sensors on the body, which can be cumbersome. Approaches for recognizing coarse subset of gestures using only a single device such as a mobile phone have also been proposed [1,22]. These approaches achieved impressive results with minimal instrumentation. Unfortunately, these approaches can only detect gestures involving body parts that are instrumented with sensors. Arguably, users prefer non body contact approach. In this work, we aim to perform unobtrusive off-body sensing that allows broader support on interaction design.

Other sensing methods such as microwaves-based approaches pose potential health and regulation problems. Simple pyroelectric systems have very slow response times (>100 milliseconds) and can only respond to changing signals. Methods involving lasers often require scanning which are line-of-sight and may cause eye damage.

Human motion detection systems that utilize quasi-electrostatic fields generated during walking have also been proposed [14,15]. However, the detection of the quasi-electrostatic fields is strongly affected by the electromagnetic fields generated by surrounding electrical equipment. Human body models describing the phenomenon of electrical charge during walking have also been proposed [3,25,27]. These models show that motion detection using passive static EF sensing is possible with complex analog circuitry and body instrumentation.

EF sensing has been used in HCI work for sensing gestures as means of user input [7,8,10,18,21,23,30,31]. These techniques use *active* approach, requiring time-varying signal transmitter and receiver that measure the signal at different location. Consequently, these solutions pose design complexity that can lead to additional power consumption. Pioneered by Rekimoto [19] and most recently Cohn et al. [6,7], human body motion detection using static EF sensing by *passively* measuring the voltage at a location on the user's body have been proposed. Such approaches enable low-power implementation. These techniques have been relied heavily on body-mounted sense electrode/s, which poses usability issues (e.g. rigidly fixing

sense electrode/s to maintain direct contact with the skin at most of the time is difficult, and uncomfortable). Furthermore, it's technically challenging to differ the actual signal from the noise caused by sensor and skin displacement. Also, Cohn et al. in [6] proposed sensing of the voltage between the body and a small ground plane near the body, i.e. they did not have a ground reference; hence the signal was very weak such that they required heavy amplifications. Our method has a true ground reference so that the signals are much stronger. In broader interaction design point-of-view, decoupling the sense electrode from the user's body allows us to gain multitudes of interesting application domains we can explore.

We extend previous work by proposing sensing method that leverages much simpler hardware, while aggregating more stable and reliable signal. Furthermore, we also investigate multiple user differentiation and location classification using ambient EF fingerprints. We are not aware of previous work that has explicitly observed the usage of *passive (non-signal transmission)* sensing of *ambient (off-body)* static EF for HCI.

PASSIVE AMBIENT STATIC ELECTRIC FIELD SENSING

Off-Body Static EF Sensing Model

The human body is electrically charged during motion [3,24,26]. From Figure 2, the potential U_B of the human body when it is performing walking motion can be expressed as follows.

$$U_B = Q_B \frac{\varepsilon_a S + x C_B}{C_B \varepsilon_a S} \quad (1)$$

where C_B is a capacitance between the body and the environment, Q_B is the instantaneous charge of the human body during walking motion, ε_a is the permittivity of the air gap between the sole and the floor, and S is the effective sole area at a height x above the floor. The induced charge Q_e of the measurement electrode placed at a certain distance from the subject can be expressed as follows:

$$Q_e = C_d(U_B - V_e) \quad (2)$$

where C_d is the capacitance between the human body and measurement electrode, and V_e is the potential of the measurement electrode. From the Eq. (1) and (2), the induced current I_e flowing through the sensor electrode can be expressed as follows:

$$I_e = \frac{dQ_e}{dt} = C_d \frac{dU_B}{dt} = C_d Q_B \left(-\frac{x}{\varepsilon_a S^2}\frac{dS}{dt} + \frac{1}{\varepsilon_a S}\frac{dx}{dt} \right) \quad (3)$$

Assuming that the human body is a good conductor, the first term in Eq. (3) represents the current induced as the result of foot motion just before it is lifted off the floor. The second term represents the current induced as the result of foot and leg motion after the foot is lifted off the floor. Note that the second term is approximately proportional to the velocity of the foot. Therefore, in a scenario of body motion near the sensor electrode, it is possible to measure the current generated under perfect non body contact condition.

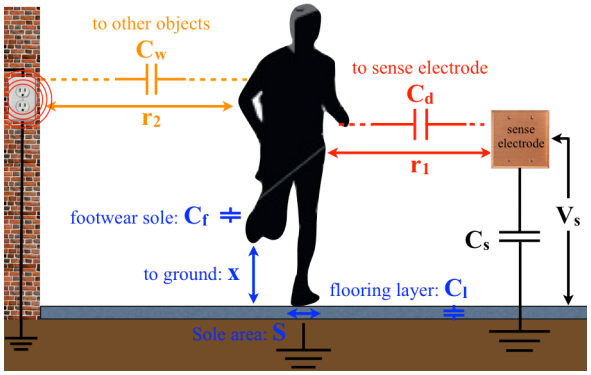

Figure 2. Circuit model of capacitive coupling between the user's body, the environment, and the sense electrode. The sensing voltage (V_s) is measured between the sense electrode and earth ground.

In practical conditions, a person walking or scuffing may develop potentials of over 1000 Volts depending on shoe sole thickness and resistance of the ground surface. Moreover, as s/he raises one foot his body capacitance to ground reaches a minimum and this in turn causes his potential to rise to a maximum. When both feet are momentarily making ground contact, the charge potential is lowest. These caused the characteristic of rise and fall in potential due to foot motion.

Sensing Parameters

A passive EF sensing is one in which the EF is generated external to the detector. If the sensor itself generates EF which is then perturbed by the object, the system is known as an active EF sensing. In this paper we deal with a passive detection system in which the ambient static EF is perturbed or distorted by the presence of an intruder (e.g. human body).

Previous work by Cohn et al. describes the theory of operation behind static electric field sensing when the device is placed on the body of the user being sensed [6]. In this previous work, a voltage is measured between the user's body and a small "local ground plane" that is located on the sensing device, but is electrical isolation from the body. In this work, the same static electric field phenomenon is leveraged, but the sensing device is not directly attached to the user's body, and therefore the important capacitances are changed as shown in Figure 2.

Firstly, we observe a capacitance C_B between the body and the environment. In Figure 2, this is separated into two capacitances: the coupling capacitance C_F between the user's feet relative to the ground, and the coupling capacitance C_w between the body and other objects in the environment, such as the walls. We assume that there are two highly resistive layers between the feet of the subject and the ground. One layer is the sole of the subject's footwear. The other is the surface of the floor. The capacitance C_F may be calculated as the sum of the capacitance C_f of the sole and the capacitance C_l of the surface of the floor. Therefore, C_B can be expressed as:

$$C_B = C_w + C_F = C_w + \frac{C_f C_l}{C_f + C_l} \quad (4)$$

Unlike the previous on-body sensing case, there is now a coupling capacitance between the body and the sense electrode (C_d), which is mostly a function of the proximity of the user to the sense electrode. The sensing unit is basically a sensor depicted as a probe or antenna of arbitrary shape connected to an ADC input of a microcontroller. It is assumed that probe's size and shape does not disturb the field being measured. Finally, the sensing voltage (V_s) is measured from the sense electrode to earth ground (i.e., across the sense capacitor C_s).

Since the sense capacitor (C_s) value is fixed, changes in any of the coupling capacitances result in an AC voltage change on the sensing voltage (V_s). For normal interactions, V_s is most affected by changes in (1) the distance between the user and the sense electrode–ΔC_d, (2) the user's contact area with the floor–ΔC_F (e.g., standing on one foot vs. two), and (3) the proximity of the user to other objects in the interaction space–ΔC_w.

IMPLEMENTATION

Hardware Approach

Previous work on sensing static electric fields required custom analog hardware to DC bias, amplify, and filter the signal before it could be sampled and used for motion classification [6,7,19]. In this work, we demonstrate the ability to sense static electric fields using simple and available commodity prototyping hardware. Our hardware implementation consisted of only an off-the-shelf microcontroller such as Arduino [4]. Arduino is a very popular embedded systems prototyping platform in the hobbyist, designer, and artist communities. Our implementation of the static electric field sensor requires no additional hardware besides an Arduino and a sense electrode, which can be made from foil.

Since we are interested in only an AC signal, we need to DC bias the signal in order to sample it using the single-ended analog-to-digital converter (ADC) on the microcontroller board. Traditionally, a DC level is established by adding a high impedance path to a reference voltage. Unfortunately, we would need an extremely large resistor value in order to avoid cutting off the 60 Hz signals we want to observe. In previous work, this was accomplished using custom hardware before the ADC.

In contrast to the previous approaches, we use a simple channel-switching method to DC bias the ADC signal (i.e. we implemented alternate-sampling of the internal voltage reference (VREF) and the analog input). In the case of Successive Approximation Register ADC, sampling the VREF will pre-charge the ADC input to a known level. This should establish a DC level when we switch back to sample the analog input (which shares that stored charge). Broad range of microcontroller boards such as Arduino incorporate Successive Approximation Register ADC in their design, due to low-cost and ease of interfacing.

Our hardware configuration requires no filtering before the ADC, because we do not utilize the raw EF samples as our main signal. Typically, when sampling low frequency EF, the extremely strong main noise (60 Hz) and it's harmonics will alias into the reading, which can cause the reading to clip as the AC amplitude becomes too high. Previous work such as [6] required hardware implementation of a low pass filter. Our approach can be implemented digitally in software, which supports easy deployment in already existing microcontroller boards.

Processing

Data acquisition

In our prototype, we used an off-the-shelf microcontroller (prototyped with ATmega 2560/328/168) and attached a sense electrode in one of its analog input. Each analog input available on the microcontroller potentially forms an EF sensor channel. Small electrode surface area may be sufficient if the sensing unit is placed near the human body, e.g. in-pocket sensing configuration. The microcontroller then stacked with lithium-ion battery pack for power, and a XBee for wireless communication to the signal processing PC. In scenarios that do not require wireless communication, the microcontroller was connected to a FTDI FT232RL USB to serial IC, thus further redirects all the communication with PC through a USB connection.

The data acquisition algorithm was implemented in AVR C firmware for the microcontroller. Each channel was sampled at 20 Hz, a sampling rate that would be considered too low for any significant noise other than EF disturbance that we are examining, but was able to represent the relevant spectrum for motion, gesture, and activity recognition. This reduced sample rate (and consequently low processing bandwidth) makes our technique readily portable to embedded processors with limited resources.

Real-time signal capture

Serial communication client written in Java was used for interfacing the sensing unit and PC. Furthermore, this program performed several other key functions. First, it provides live visualization of the data from our sensor/s, which is useful to identify distinctive features for analysis.

A single packet of our raw data stream consisted of a 10-bit sample of sense electrode reading (Figure 3, red line), and offset *ó* (Figure 3, yellow line, multiplied by 100 for better visualization). We defined *ó* as a ratio of ideal and actual VREF reading when measured against Vcc. It essentially shows very small fluctuations in Vcc. We accommodate these small fluctuations in our measurements to have more accurate ADC readings. In the case of ATmega 168/328, VREF is 1.1 V and Vcc is 5 V, hence:

$$ó = \frac{\frac{1.1}{5} \times 1023}{VREF\ reading} = \frac{225.06}{VREF\ reading} \quad (5)$$

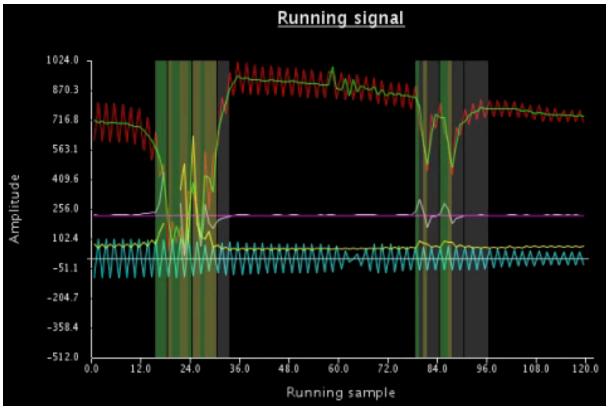

Figure 3. Signal acquisition in *Mirage*, showing raw sample (red line), DC component (green line), AC component (blue line), main signal (white line), event detection (green and yellow highlights) and gesture segmentation (grey highlights).

Our first treatment to the raw sense electrode reading was to apply a 3rd order Butterworth IIR low-pass filter with a 3 dB corner at 7 Hz. This filter reduces the high frequency component (higher than 7Hz) of sampled signal (Figure 3, green line). The DC waveform is then multiplied with *ó*. After multiplying the DC waveform with *ó*, we aggregate our signal that fluctuates relative to the magnitude of user's movements. This signal is plotted in Figure 3 (white line).

From the raw data stream (Figure 3, red line) we can also examine that the amplitude of the AC components also changes significantly during a gesture. This is mainly caused by changes of proximity between the body and electromagnetic sources in the environment (ΔC_w in Figure 2), in addition to changes in the frequency response. We extracted the AC components by applying a 3rd order Butterworth IIR high-pass filter with a 3 dB corner at 7 Hz to our raw data stream. The AC component of our signal is plotted in Figure 3 (blue line). To capture the AC amplitude in this signal, we compute the root-mean-square (RMS) over each window.

Analysis

To give a clear target on the signal features we need to explore, we focused our activity and gesture recognition study in the following domains:

1. Continuous activity recognition
   This domain focuses to recognize relatively long-duration activities. These problems generally have the property of using relatively long windows (since activities don't change rapidly) and not focusing on individual events. In this paper, we test our sensing approach to recognize when the user is standing still, walking, running, or doing jumping jacks.
2. Discrete activity recognition
   This domain focuses on repeated events, which have more tolerance to false negatives. In our study, we perform activity counting and activity density calculation (e.g. step per-second) from the aforementioned continuous activities (walking, running, and jumping jacks).
3. Gesture recognition
   This domain focuses on recognizing discrete command gestures, which generally have the properties of occurring slowly and infrequently, with high cost of false positives and false negatives. We investigate the feasibility of our system to detect, segment, and classify whole-body gestures.

Based on the aforementioned activity and gesture recognition targets, we implemented necessary signal analysis approaches such as event detection (including counting), gesture segmentation, feature extraction, and gesture classification.

Real-time event detection

In this stage, we aimed to detect real-time events of EF disturbances mainly caused by body movements to perform continuous and discrete activity recognition. Our system incorporates heuristic based adaptive threshold approach to detect these events. This simple approach is sufficient and effective for our signal mainly because the aggregated signal is clean, stable, and has predictable behavior. The signal rise and fall (as illustrated in Figure 3 by light green and light yellow highlights, also shown in Figure 7 and 8a) were direct effects of foot lift and foot land. Hence, continuous activities such as walking, running, jumping jacks, or standing still can be inferred simply by analyzing the signal amplitude and frequency. Our step-counting algorithm is based on threshold crossings, with rejection of crossings that are too close in time.

Real-time segmentation

Next, the program segmented inputs from the data stream into independent instances. Our system requires a real-time segmenter that automatically identifies gesture events from the live signal stream. We used similar adaptive thresholding method as the event detection described above, and then compute finite difference (i.e. sample-to-sample difference) of the signal in 1-second non-overlapping window. We set 1-second window because the designated gestures are unlikely to exceed 1-second period. By implementing this, the latency of our real-time segmentation algorithm is purely limited to sampling time (group delay of low pass filter). The mean value of the computed finite difference is then compared to a dynamic threshold aggregated from the adaptive algorithm similar to that implemented in our real-time event detection; if the absolute value of the mean is greater than the threshold, the system considers the current instance to be a gesture. The real-time segmentation results are illustrated in Figure 3 marked by light grey highlights.

Real-time feature extraction

In this stage, the program analyzed segmented signals and performs feature extractions. Below are the 77 features we exploited for our gesture classification:

- Signal waveform (20, Figure 3 – white line).
- DC & AC waveform (40, Figure 3 – green and blue line)
- Mean (1): average value of the signal over the window
- Median (1): the median signal value over the window
- Standard Deviation (1): the spreadness of the signal over the window
- Variance (1): the square of standard deviation
- Root Mean Square (1): The quadratic mean value of the signal over the window
- Zero Crossing Rate (1): The total number of times the signal changes from positive to negative or back or vice versa normalized by the window length
- Mean Crossing Rate (1): The total number of times the signal changes from below average to above average or vice versa normalized by the window length
- Signal spectrum (10): 20-points FFT of the signal.

Real-time classification

Our system classified these input instances into a set of gestures using Sequential Minimal Optimization (SMO) implementation of the Support Vector Machine (SVM) classifier found included in the WEKA [11]. Our system runs the new features against a previously trained model to produce gesture classification results.

Resolution and Signal-to-Noise Ratio

In the current configuration, our sensor has an update rate of 20 Hz. This is considered sufficient because we are dealing with body movements which are not likely to exceed 10 Hz. It is important to note that our system is capable of performing much higher refresh rate, but at the same time we also focused on reducing unnecessary data transfer to perform ultra-low power sensing.

Our sensing method passively measures noise in electric field due to body motion. To evaluate our signal, we choose the alternative Signal-to-Noise Ratio (SNR) definition, which is a reciprocal of the coefficient of variation of a set of samples taken over a period of time. We collected an hour-long sample of our signal and measured the mean and standard deviation. The mean was 224.65 (SD=2.59), hence the SNR is:

$$SNR = \frac{\mu}{\sigma} = \frac{224.65}{2.59} = 86.74 \qquad (6)$$

Note that our measurement includes variations from nearby electrical appliances, and also from the presence of experimenter who was standing still near the sense electrode during the data collection. This measurement scenario closely resembles actual usage scenario of *Mirage*.

EVALUATION

We designed and carried out a series of experiments to investigate the usability of our sensing approach, as well as to establish the baseline performance of the recognition engine. The experiment was conducted in 10 separate locations in 2 different office buildings. The office buildings had 4 and 3 floors with basements. We selected these locations to represent different flooring materials, building constructions, and surrounding electrical appliances, thus form a wide variety of ambient static EF. For a single location, experiments were conducted in a single visit.

Our participants were unique for every location, totaling in 10 participants (3 female), weighed between 47 and 84 kg (mean=65 kg), and height between 163 and 184 cm (mean=172 cm). Throughout our experiments, we did not require participants to use certain footwear. However, we did suggested participants to wear shoes, i.e. not barefooting. During our experiments, we avoid non-participants from entering the experiment space.

Activity Recognition

Setup

We developed a system that acquires signals produced by *Mirage* sensor, detects when a user is present, and recognize the amount and type of user's activity. To test the robustness of this system, we conducted evaluations where the participants in different locations performed the following activities: (1) participant not in the room, participant in the room and (2) standing still, (3) walking, (4) running, and (5) jumping.

To support these scenarios, we attached a 50 × 5 mm copper tape as our sense electrode on the notebook PC monitor frame and our microcontroller was connected to the notebook PC by USB cable (similar setup as Figure 4a, but attached on notebook PC monitor). The notebook PC was powered by internal li-ion battery.

Procedure

We instructed the participants to subsequently perform each of the designated activities for 10 seconds period at the

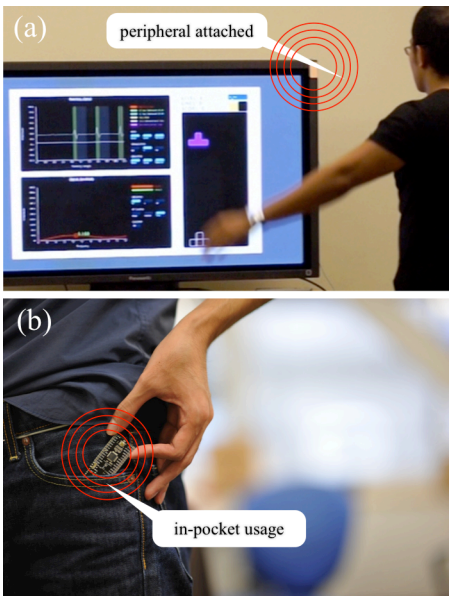

Figure 4. Setup used in our evaluation: (a) microcontroller with sense electrode attached to a monitor frame, and (b) microcontroller (with wireless connection) without additional sense electrode for in-pocket usage.

same location in the experimental space (i.e. without locomotion). In general, our signal exists regardless of locomotion. Participants performed activities within the sensible distance from the sensor (typically <2m). We also instructed the participants to count their steps during walking, running, and jumping activities. Participants then reported their counting results to the experimenter. We repeated this session 5 times for each of the participants. Overall, we obtained 250 samples.

The real-time event detection was done automatically during each session. Our system logs signal peaks and valleys together with their amplitudes, as well as signal frequencies obtained by spectral analysis (FFT). Combined, these data served as features for activity recognition. In this experiment, we set static thresholds for the aforementioned features to identify activities; therefore our activity recognition system does not require training.

Results

By comparing the aggregated activity recognition results with the ground truth data, we obtain 96.72% average accuracy (SD=5.35%) across 5 activities for 10 participants. Note that we used heuristic threshold to identify activities in a simple, low-power, and fast way (in contrast to machine learning based approaches), which can be extended to leverage more advanced recognition algorithm for supporting broader type of activities.

Furthermore, we compared the automated and self-reported step counting results; yielding an average of 8.41% error margin (SD=3.12%). Note that high-quality research grade pedometers available in the market have typical error margin of ±5% [5,22]. These results seem promising with plenty of headroom for fine-tuning.

Gesture Classification

Setup

To aggregate whole-body gestures, we extended our activity recognition system (which is basically a real-time event detection and heuristic threshold setting) with real-time segmentation, feature extraction, and SMO based classifier. We used the techniques described in the previous section. To evaluate this system, we recruited the same participants and adopted similar setup as our previous experiment. The designated gestures include: (1) left arm lift, (2) right arm lift, (3) left hand rotation, (4) right hand rotation, and (5) jump. We illustrate these gestures in Figure 5.

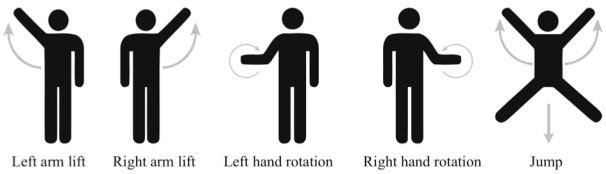

Figure 5. Stick figures describing the 5 gestures performed by participants in our gesture classification experiment.

Procedure

First, the participants were instructed to train themselves to perform the gestures. Soon after, the participants were instructed to subsequently perform each of the gesture for 5 times. To avoid over fitting, we treat the aforementioned session as one fold, and then we repeated the session for 5 times (5-fold). Overall, we aggregated 1250 samples of gestures. Our system performs segmentation and feature extraction automatically. It labeled and recorded each sample for our 5-fold cross-validation test. Prior to the test, we trained our SMO classifier in user dependent manner.

Results

The average accuracy across 10 participants and locations was 92.11% (SD=6.84%) when classifying between 5 gestures. These results are encouraging for explorations on inferring gestures from completely passive static EF sensing using no body contact approach. It also validate our assumption that *Mirage* would work equally well across a reasonably wide set of people and homes.

Location Classification

Setup

We conducted a study on location classification based on our hypothesis that different environments will give different fingerprints of ambient EF features. This is mainly caused by the variation of electrical appliances and electricity wiring that acts as electromagnetic sources. To be able to see wider range of the spectrum, we modified our sampling mechanism to sample only from the sense electrode. In this experiment, we sampled our ADC at 400 Hz, resulting in a spectrum width of 200 Hz, easily containing 60 Hz mains and its harmonics.

We measured EF fingerprint in 6 locations: (1) work desk, (2) meeting room, (3) kitchen, (4) hallways, (5) hardware lab, and (6) soccer field. The examples of the signals for each location are available in Figure 6. This ambient EF reading confirmed our hypothesis on the variability of EF fingerprints across different locations.

We recruited the same participants as previous experiments. The sensor was placed in the user's pocket, with no additional electrode attached to the analog input of the microcontroller (Figure 4b). This usage scenario works well to capture the EF fingerprint mainly because the human body acting as an antenna receives wide-range of frequency from the environment. Moreover, the analog input in close proximity to the body picks significantly stronger signal (ΔC_d in Figure 2).

Procedure

We instructed the participants to freely choose a spot at above locations, and remember it for the next round of data collection. Each location of every round naturally separated in time due to participants moving from one location to another. Hence the training and testing data were from the relatively same spot, but separated in time.

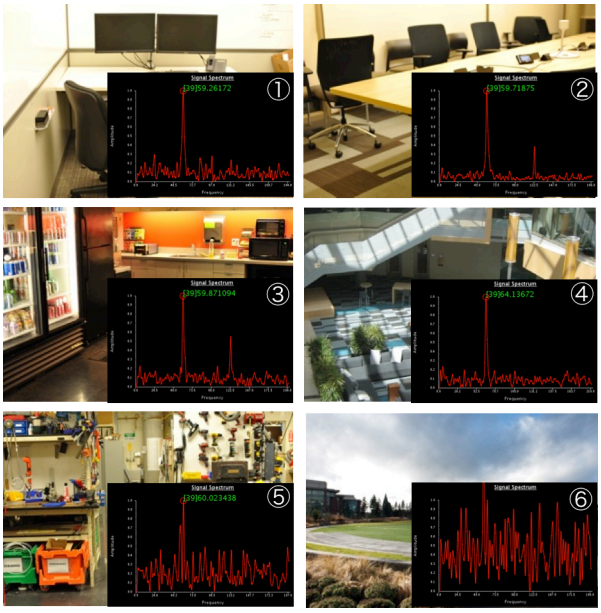

Figure 6. The ambient electric field fingerprints sampled from 6 different locations show distinctive features that we leveraged in our location classification.

At the measurement location, participants pressed a keyboard key to start collecting 100 samples of EF fingerprints (each consists of spectral features), which took approximately 100 seconds. We subsequently perform the data collection for all the locations and repeat it again for 5 rounds. Overall, we aggregated 30000 samples that were trained in user dependent manner.

Results

We performed 5-fold cross validation using our SMO classifier. The average accuracy was 98.12% (SD=4.47%) when classifying between 6 locations. This is impressive, given that the approach was simple, and there is still plenty of headroom to fine-tune the parameters.

Multiple User Differentiation

Setup

We conducted a study to leverage 2-channel *Mirage* sensor and Independent Component Analysis (ICA) algorithm to differentiate signal source coming from multiple user. In this experiment, we used the same implementation as our activity recognition, except that we had utilized two-channel *Mirage* sensor and applied ICA to the signals.

Procedure

We instructed 2 participants to perform foot motion (without locomotion) in a 2 × 2 m work desk cubicle. We also asked the participants to perform foot motion in different speeds relative to each other.

We applied our ICA based multiple user differentiation approach to the real-time signal. We observe the behavior of the signals and the aggregated independent components.

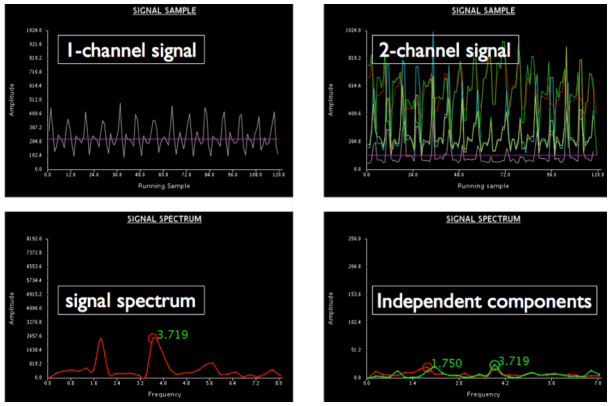

Figure 7. Multiple users differentiation using Independent Component Analysis (ICA). Upper left graph shows mixtures of signals captured by 1-channel sensor, and consequently mixed spectrum as shown in lower left graph. Using two-channel sensor and implementing ICA separates the independent components of the signal, revealing two signal sources as shown in lower right graph.

Results

Our system successfully aggregated independent components of the signals originated from 2 participants. We show an exemplary result in Figure 7, where a participant was walking and another participant was running.

Combining ICA with simple amplitude based proximity sensing has the potential to help multiple user tracking. ICA can also be used to filter out noise from the signal, especially in the crowded environment. Exploring user tracking and noise filtering using ICA remains future work.

Interactive Application

We developed three applications to demonstrate *Mirage* real-time interactive capabilities. The first application shows the capability of *Mirage* to perform activity monitoring. This application provides real-time visualization of the raw data stream, results of the signal processing (AC/DC components, signal, FFT of the signal) as well as context aggregation results such as standing still, walking, running, and jumping, with their respective speeds and step counts (Figure 8a).

The second application leverages activity detection to control the movement of a game character. Figure 8b shows a user playing the game where he tries to avoid obstacles by walking, running, and jumping.

The third application is a Tetris game, which the user controls were mapped to a player's whole-body gestures. Although a wide range of gestures can be trained, we leverage intuitive arm and foot motions such as: lifting left or right arm for left or right movement respectively, rotation gesture with one hand for Tetris block rotation, and jumping gesture to drop the block on the top of the stacks. In this application, we pre-trained the gesture classifier

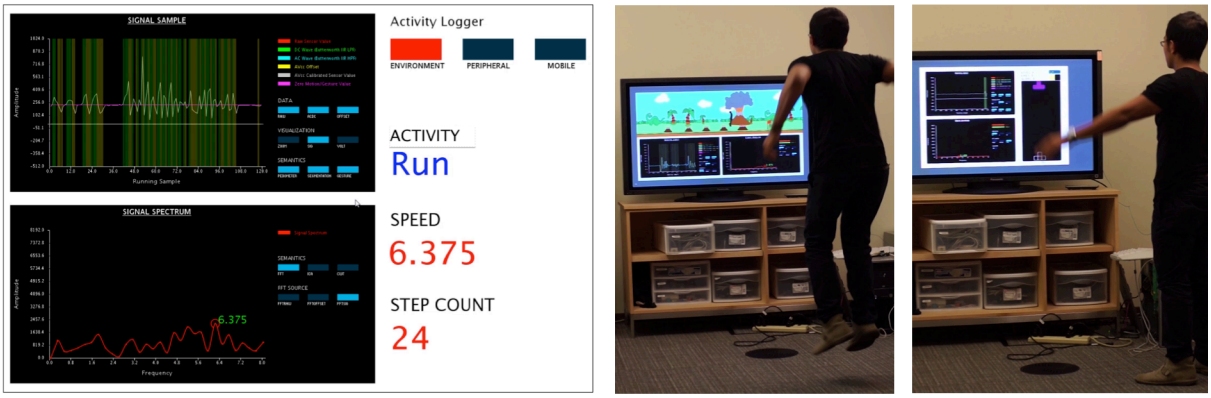

(a) Activity monitoring (b) Avatar-control game (c) Tetris game

Figure 8. Our interactive applications build on: (a) continuous and discrete activity recognition for activity monitoring, (b) discrete activity recognition embedded in an avatar-controlling game where a user has to physically walk, run, or jump to avoid obstacles, and (c) gesture recognition embedded in a Tetris game where user controls are mapped to whole-body gestures.

(SMO) using 10 examples of each gesture. Figure 8c shows the actual image of a user playing our Tetris game.

DISCUSSION

Through the experiments presented in this paper, we have shown that using the proposed off-body static electric field sensing, our system is able to perform activity recognition, gesture recognition, location classification, and multiple user differentiation in encouraging results. In addition, by developing three interactive applications we have demonstrated the ability to run our system in real-time. This section discusses the limitations of the current system, and future work to improve the system.

Limitations and Future Work

The EF strength E at a distance r away from a point charge Q is given by:

$$E = k\frac{Q}{r^2} \qquad (7)$$

where k is Coulomb's Law constant ($9.0\times10^9 N\,m^2/C^2$). Hence, the EF strength is inversely proportional to the square of the distance. Consistent with this, the sensitivity of our sensing approach is limited to a certain distance from the subject to sensor (ΔC_d in Figure 2). Fortunately, depending on the usage scenario this limitation can also be a *feature*. Limiting sensible space helps to avoid noisy signal, and useful to recognize events only from users who are nearby the sensors. This can also be a hint for proximity sensing. Also, by leveraging spatially distributed sensors we can upscale the usage to indoor location estimation.

Circuit model represented in Figure 2 and physics model represented in Eq. (1-4) note that the capacitance of the foot to the ground (C_F) and the body to nearby objects (C_w) influence the resulted sensing voltage (V_s). Hence, the resistance of user's footwear also highly influences the magnitude of our signal (i.e., the higher the resistance, the higher magnitude of the signal our system can capture). While we do not have exact solution for this particular limitation yet, our pilot experiments showed wide-range of footwear could produce detectable signal. Furthermore, our heuristic-base adaptive threshold approach also helps to detect marginal changes in the signal for further processing.

From the physics model represented in Eq. (2), capacitance between body and sense electrode (C_d) is directly proportional to the induced charge of the measurement electrode. Thus, the area size of the sense electrode also influences the magnitude of our signal (bigger electrode yields more sensitive system). Fortunately, using Mirage as a mobile sensor (e.g. in-pocket usage scenario) will mitigate this limitation; i.e., if the distance between the sensor and subject decrease, the signal magnitude will increase significantly. Using Mirage as peripheral attached sensor or environmental sensor also gives more headroom for attaching larger sense electrode.

For future iteration of this work, we plan to explore the interaction design space for *Mirage* in mobile devices, as well as exploring integration of *Mirage* in homes (interfacing with powerline). Also, we plan to further explore our multiple user differentiation to support multiple user tracking.

CONCLUSION

In this paper, we have presented a novel approach to infer the amount and type of motion, gesture, and activity, as well as location classification and multiple user differentiation using non body contact and passive static electric field sensing, namely *Mirage*. We have described the theory of operation and detailed implementation of the sensing system that leverages the design of ADC in off-the-shelf microcontrollers, which allows simple setup with no instrumentation on the user. *Mirage* systems can be extremely small, lightweight and low power. Since electric fields penetrate non-conductors, electrode sensors can be hidden, providing protection from weather and wear, while simultaneously adds the element of disappearing input interface. *Mirage* also works outdoor, enabling truly mobile solution. Results from our experiments have demonstrated that our system performs reasonably well for a series of

activity and gestures. Additionally, we have presented results on location classification within a building and outdoor, as well as multiple user differentiation using ICA. We conclude with demonstration of an activity monitoring application, and two interactive applications showing immediate applicability and rich interaction design space enabled by *Mirage*.

ACKNOWLEDGEMENTS

We are thankful to Desney S. Tan, Shwetak N. Patel, and Gabe Cohn for their significant contribution in helping to understand passive electric field sensing and its principles of operation. We also thank anonymous reviewers for their thoughtful comments and subjects who participated in the experiments. This work is partially supported by Microsoft Research through Collaborative Research (CORE) Projects.

REFERENCES

1. Agrawal, S., Constandache, I., Gaonkar, S., Choudhury, R., Caves, K, DeRuyter, F. Using Mobile Phones to Write in Air. *Mobisys 2011,* 15–28.
2. A. Mansfield, and GM. Lyons. The Use of Accelerometry to Detect Heel Contact Events for Use as a Sensor in FES Assisted Walking. *Med. Eng. Phys.*, Vol. 25, pp. 879–885, 2003.
3. A. Ohsawa. Electrostatic Characterization of Antistatic Floors Using an Equivalent Circuit Model. *Journal of Electrostatics*, Vol. 51–52, pp. 625–631, 2001.
4. Arduino. http://arduino.cc/
5. C G Ryan, P M Grant, W W Tigbe, M H Granat (2006). The Validity and Reliability of a Novel Activity Monitor as a Measure of Walking. *British Journal of Sports Medicine*, 40 (40): 779–784.
6. Cohn, G., Gupta, S., Lee, T., Morris D., Smith J.R., Reynolds, M.S., Tan D.S., Patel S.N. An Ultra-Low-Power Human Body Motion Sensor Using Static Electric Field Sensing. *Ubicomp '12*, 99–102.
7. Cohn, G., Morris, D., Patel, S.N., Tan, D.S. Humantenna: Using the Body as an Antenna for Real-Time Whole-Body Interaction. *CHI '12,* 1901–1910.
8. Dietz, P. and Leigh, D. DiamondTouch: A Multi-User Touch Technology. *UIST '01*, 219–226.
9. FitBit. http://www.fitbit.com/
10. Fukumoto, M. and Tonomura, Y. Body coupled FingeRing. *CHI '97*, 147–154.
11. Hall, M., Frank, E., Holmes, G., Pfahringer, B., Reutemann, P., Witten, I.H. The WEKA Data Mining Software: An Update. *SIGKDD Explorations*, 11.1 (2009).
12. JRW. Morris. Accelerometry a Technique for the Measurement of Human Body Movements. *Journal of Biomechanics*, Vol. 6, pp. 729–739, 1973.
13. Junker, H., Lukowitz, P., Troester, G. Continuous Recognition of Arm Activities with Body-Worn Inertial Sensors. *ISWC '04,* 188–189.
14. K. Takiguchi, T. Wada, and S. Toyama. Human Body Detection that Uses Electric Field by Walking. *Journal of Advanced Mechanical Design, Systems, and Manufacturing*, Vol. 1, No. 3 pp. 294–305, 2007.
15. K. Takiguchi, and S. Toyama. Does a Dog Recognize his Master by an Electric Field? Generation and Transmission of an Electric Field Around a Walker. *Journal of International Society of Life Information Science*, Vol. 21, No. 2, pp. 428–433, 2003.
16. Michoud, B., Guillou, E., Bouakaz, S. Real-time and markerless 3D human motion capture using multiple views. *In Proc of Human Motion 2007*, 88–103.
17. Nike+. http://nikeplus.nike.com/plus/
18. Rekimoto, J. GestureWrist and GesturePad: Unobtrusive Wearable Interaction Devices. *ISWC '01*, 21–27.
19. Rekimoto, J. and Wang, H. Sensing GamePad: Electrostatic Potential Sensing for Enhancing Entertainment Oriented Interactions. *CHI EA '04*, 1457–1460.
20. R. Williamson, and BJ. Andrews. Detecting Absolute Human Knee Angle and Angular Velocity Using Accelerometers and Rate Gyroscopes. *Med. Biol. Eng. Comput*. Vol. 39, pp. 1–9, 2001.
21. Sato, M., Poupyrev, I., Harrison, C. Touché: Enhancing Touch Interaction on Humans, Screens, Liquids, and Everyday Objects. *CHI '12,* 483–492.
22. Scott, J., Dearman, D., Yatani, K., Truong,K.N. Sensing Foot Gestures from the Pocket. *UIST '10*, 199–208.
23. Smith, J.R. Field mice: Extracting hand geometry from electric field measurements. IBM Systems Journal, (35) 3.4, 1996, 587–608.
24. Susan D. Vincent, Cara L. Sidman. Determining Measurement Error in Digital Pedometers. *Measurement in Phys. Ed. and Exercise Science*, 7 (1): 19–24. 2003.
25. T. Ficker. Electrification of Human Body by Walking. *Journal of Electrostatics*, Vol. 64, pp. 10–16, 2006.
26. Vicon. http://www.vicon.com
27. V. Amoruso, M. Helali, and F. Lattarulo. An Improved Model of Man for ESD Application. *Journal of Electrostatics*, Vol. 49, pp. 225–244, 2000.
28. Wachs, J., Kölsch, M., Stern, H., Edan Y. Vision-based hand-gesture applications. *In Comm. ACM* 54.2, 60–71.
29. Xbox Kinect. http://www.xbox.com/en-US/kinect
30. Zimmerman, T.G. Personal Area Networks: Near-Field Intra-Body Communication. *IBM Systems Journal,* (35) 3.4, 1996, 609–617.
31. Zimmerman T.G., Smith J.R., Paradiso J.A., Allport D., Gershenfeld, N. Applying Electric Field Sensing to Human-Computer Interfaces. *CHI '95,* 280–287.